Thermal Electron Flow in a Planar Crossed-Field Diode

David Chernin, Abhijit Jassem, and Y. Y. Lau, *Fellow, IEEE*

***Abstract*— A self-consistent model of steady-state electron flow in a planar crossed-field diode with a thermionic cathode is presented. Our formulation is a generalization of the classic work of Fry and Langmuir, to include a constant magnetic field B of arbitrary strength parallel to the electrode surfaces. Some effects of the magnetic field on the electron flow are illustrated in an example.**

***Index Terms*— Crossed-field diode, Hull cutoff, space charge limited, temperature limited, thermionic emission.**

I. Introduction

THERMIONIC cathodes are widely used as electron sources. In a diode, as the cathode temperature is raised, the anode current transitions from the temperature-limited value, which is described by the Richardson–Dushman law [1], [2] to the space charge-limited value, which is described by the Child–Langmuir law [3], [4]. The 1-D theory of this transition is given in the classic articles by Langmuir [4] and Fry [5], who found that, above a certain transition temperature, the anode current is controlled by the appearance of a potential minimum in front of the cathode. This potential minimum is also known as a virtual cathode [6]–[8]. We recently extended the 1-D theory of Fry and Langmuir to 2-D in order to study various effects of nonuniform emission [9]. This work was motivated by our attempt to understand the physical basis for the shape of the Miram curve [10], which is a plot of the anode current as a function of the cathode temperature at a fixed voltage. The Miram curve usually exhibits a smooth "knee" which marks the transition from the temperature-limited regime to the space charge-limited regime. Operation in the knee region is often chosen for stability and long cathode life.

Much less developed is the thermionic theory of a crossed-field diode, in which an external magnetic field B is imposed parallel to the cathode surface. The anode current depends on the value of B, in addition to the space charge density. The anode current quickly approaches zero once B approaches and exceeds a value known as the Hull cutoff, B_H [11].

The theoretical analysis of current transport in a diode with a transverse magnetic field is surprisingly subtle [6], [12]–[14]. Consider, for example, a model in which the emission velocity of all electrons is zero. The maximum emitted current that permits time-independent solutions for $B < B_H$ is obtained by setting the cathode surface electric field $E_C = 0$ [6], [12]. However, the limiting current for $B > B_H$ always occurs when $E_C < 0$, corresponding to initial acceleration of electrons [13], [15]. The maximum injection current for $B > B_H$ is not known *a priori* and must be calculated numerically; its existence has been confirmed in particle-in-cell (PIC) calculations [13]–[15]. The critical current is always *larger* than the value obtained by assuming $E_C = 0$. The maximum injection current is a discontinuous function of B at $B = B_H$ because the local space charge density is due only to the outward-moving electrons if B is slightly less than B_H, but is due both to outward-moving and returning electrons, if B is slightly greater than B_H [12], [13].

Current transport in a crossed-field diode is most frequently analyzed under the assumption of mono-energetic electron emission velocity. Additional assumptions, such as zero electric field on the cathode surface, are sometimes introduced [12], [13], [15]–[18]. These idealized assumptions allow simultaneous, steady-state solutions to the Poisson equation, the force law, and the continuity equation to be obtained. We are not aware of any theory of a crossed-field diode for a thermal distribution of emission velocities, similar to that developed by Fry [5] and Langmuir [4], where the space charge effect is solved self-consistently with the orbital motion. In this article, we generalize the theory of Fry [5] and Langmuir [4] to a simple crossed-field diode, including a magnetic field of arbitrary strength.

Our study of crossed-field flows below and above the Hull cutoff is applicable to the high-power microwave device known as the magnetically insulated liner oscillator (MILO) [19] and to the linear transformer driver (LTD) [20], which has recently emerged as a basic unit in the architecture of modern pulsed-power systems. Depending on the operating parameters, both the MILO and LTD exhibit a spatial region in which B transitions through B_H.

This article is organized as follows: Section II outlines the theoretical formulation that extends the 1-D theory of Fry [5] and Langmuir [4] to a crossed-field diode. Section III presents numerical solutions of the model equations for

Manuscript received July 2, 2020; accepted August 9, 2020. Date of current version September 11, 2020. This work was supported in part by the Defense Advanced Research Projects Agency (DARPA), in part by the Air Force Office of Scientific Research (AFOSR), in part by the Office of Naval Research (ONR), and in part by the L3Harris Electron Devices Division. The views, opinions and/or findings expressed are those of the authors and should not be interpreted as representing the official views or policies of the Department of Defense or the U.S. Government. Approved for Public Release, Distribution Unlimited. The review of this article was arranged by Senior Editor C. A. Ekdahl. *(Corresponding author: David Chernin.)*

David Chernin is with Leidos Inc., Reston, VA 20190 USA (e-mail: david.p.chernin@leidos.com).

Abhijit Jassem and Y. Y. Lau are with the Department of Nuclear Engineering and Radiological Sciences, University of Michigan, Ann Arbor, MI 48109-2104 USA.

Color versions of one or more of the figures in this article are available online at http://ieeexplore.ieee.org.

Digital Object Identifier 10.1109/TPS.2020.3017715

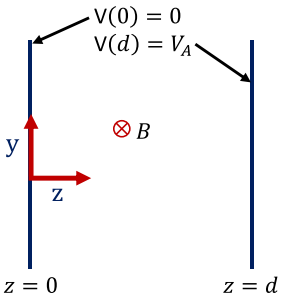

Fig. 1. Planar crossed-field diode.

values of the magnetic field B from 0 to $B_{\rm H}$ and beyond. Section IV provides a comparison with PIC simulations. We summarize our results in Section V.

II. Theory

We consider electron flow in the simple planar crossed-field diode illustrated in Fig. 1. Electrons are emitted from a thermionic cathode located at $z = 0$ and are collected at the anode located at $z = d$. We assign the potential of the cathode to be 0 and that of the anode to be $V_{\rm A} \geq 0$. A constant magnetic field B is applied in the x-direction.

We will assume that the charge density and the electrostatic potential depend only on z, but that the electrons themselves move in both the y- and z-directions. We take the electron distribution function to be given by

$$f(v_y, v_z; z) = f_2 e^{-E/kT} = f_2 e^{-(\frac{1}{2}mv_y^2 + \frac{1}{2}mv_z^2 + qV(z))/kT} \quad (1)$$

where f_2 is a normalization constant, E is the total energy of an electron, m is the electron mass, q is the electron charge, k is Boltzmann's constant, T is the cathode temperature, and $V(z)$ is the electrostatic potential. Since E is a constant of motion, f is a solution of Vlasov's equation. We assume here that all electron velocities are nonrelativistic.

We choose the value of the normalization factor f_2 by requiring that the emitted current density be the local Richardson–Dushman current density

$$\int_{-\infty}^{\infty} dv_y \int_0^{\infty} dv_z v_z f(v_y, v_z; 0) = J_{\rm RD} = AT^2 {\rm e}^{-\phi/kT} \quad (2)$$

where A is the Richardson coefficient and ϕ is the cathode work function. Carrying out the elementary integral in (2), we find

$$f_2 = \frac{1}{(2\pi)^{1/2} v_{\rm th}^3} J_{\rm RD} \quad (3)$$

where we have defined the thermal velocity $v_{\rm th} \equiv (kT/m)^{1/2}$.

The charge density $\rho(z)$ that appears in Poisson's equation is given by

$$\rho(z) = -\iint dv_y dv_z f(v_y, v_z; z) \quad (4)$$

where the ranges of integration in (4) are the velocities of electrons that reach z. In order to determine these ranges, we must consider the motion of the electrons in some detail.

Electron motion is constrained by two constants of motion, the total energy E defined in (1), and the canonical momentum in the y-direction, which may be written as

$$P_y \equiv m(v_y + \Omega z) \quad (5)$$

where $\Omega \equiv -qB/m$. Combining these, we find

$$v_z^2 = v_{z0}^2 + 2v_{y0}\Omega z - \Omega^2 z^2 - 2\frac{q}{m}V(z) \quad (6a)$$

$$v_y = v_{y0} - \Omega z \quad (6b)$$

where v_{y0} and v_{z0} are the initial values of velocity of an electron at the cathode. Using (6a) and (6b), we may change the variables of integration in (4) from (v_y, v_z) to (v_{y0}, v_{z0}). The result, which we write in terms of dimensionless variables, is

$$\bar{\rho}(\bar{z}) = \iint du d\xi \frac{e^{-(\frac{u^2}{2} + \xi)}}{(\xi - \xi_0(u; \bar{z}))^{1/2}} \quad (7)$$

where we have defined the dimensionless quantities

$$\bar{\rho}(\bar{z}) \equiv \rho(z)/\rho_0 \quad (8a)$$

$$\bar{z} \equiv z/d \quad (8b)$$

$$u \equiv v_{y0}/v_{\rm th} \quad (8c)$$

$$\xi \equiv \frac{1}{2}(v_{z0}/v_{\rm th})^2 \quad (8d)$$

where $\rho_0 \equiv -J_{\rm RD}/(2\pi^{1/2} v_{\rm th})$ in (8a). We also define the dimensionless function

$$\xi_0(u; \bar{z}) \equiv -u\bar{\Omega}\bar{z} + \frac{1}{2}\bar{\Omega}^2\bar{z}^2 - \alpha\bar{V}(\bar{z}) \quad (9)$$

where

$$\bar{\Omega} \equiv \Omega d/v_{\rm th} \quad (10a)$$

$$\alpha \equiv -qV_{\rm A}/kT \quad (10b)$$

$$\bar{V}(\bar{z}) \equiv V(z)/V_{\rm A}. \quad (10c)$$

The function $-\xi_0(u; \bar{z})$ is important. It acts as an effective potential for electron motion in z. Analysis of this function determines the limits on the integrals in (7), which are the ranges of initial velocities $(u; \xi)$ such that a particle reaches $\bar{z}$, as shown in the Appendix. We note that a particle may be turned around after it leaves the cathode by either a reversed electric field or by the magnetic field. These effects are both included in the effective potential $-\xi_0(u; \bar{z})$.

Poisson's equation may be solved numerically for $\bar{V}(\bar{z})$ using an iterative algorithm similar to that described in Appendix B of [9]. Once $\bar{V}(\bar{z})$ is known, the current density at the anode is given by

$$J_{\rm A} = \frac{J_{\rm RD}}{(2\pi)^{1/2}} \int_{-\infty}^{\infty} du e^{-(u^2/2 + \xi_1^-(u;1))} \quad (11)$$

where the function $\xi_1^-(u; \bar{z})$ is defined in the Appendix. The current density returning to the cathode is just the difference

$$J_{\rm ret} = J_{\rm RD} - J_{\rm A} \quad (12)$$

since an emitted electron either reaches the anode or returns to the cathode in this model.

Results from the numerical solution of this model are illustrated and discussed in Section III.

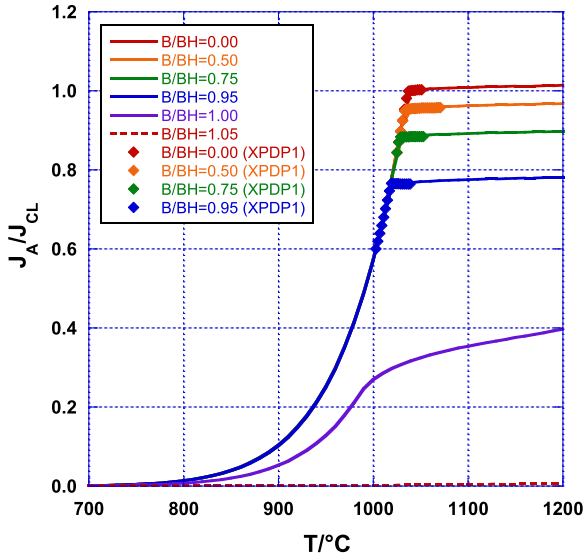

Fig. 2. Anode current density normalized to the Child–Langmuir current density $J_{\rm CL}$ [see (14)] versus temperature for various values of $B/B_{\rm H}$. Solid lines are from the numerical solution of the Vlasov–Poisson equations; "diamond" data points are from the XPDP1 PIC simulation code as described in Section IV.

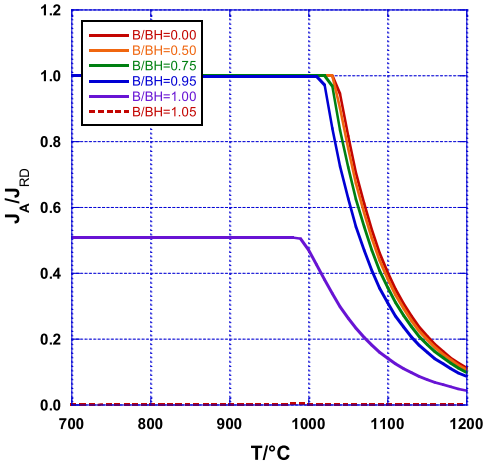

Fig. 3. Anode current density normalized to the emitted current density $J_{\rm RD}$ [see (2)] versus temperature for various values of $B/B_{\rm H}$.

III. Numerical Results

We use the same nominal values of $V_{\rm A}$ and d as in [9], namely $V_{\rm A} = 179.5$ V and $d = 0.381$ mm. We fix the work function $\phi = 2$ eV and study the effects of the magnetic field.

Fig. 2 shows the normalized current density at the anode as a function of temperature for various values of $B/B_{\rm H}$, where $B_{\rm H}$ is the Hull cutoff field [11]

$$B_{\rm H} = \frac{1}{d}\left(\frac{2mV_{\rm A}}{-q}\right)^{1/2} \tag{13}$$

which evaluates to 0.1186T for our parameters.

We see that significant amounts of current reach the anode for $B/B_{\rm H} = 0.95$, and even for $B/B_{\rm H} = 1$, but observe that the anode current drops very quickly as B is increased toward and beyond $B_{\rm H}$ (see also Fig. 7). The classical expression for $B_{\rm H}$ in (13) is derived assuming zero emission velocity, not a Maxwellian distribution, at the cathode, so we expect that $B/B_{\rm H}$ must be slightly larger than 1 for cut off of the electron flow to the anode.

The anode current density in Fig. 2 is normalized to the classical Child–Langmuir current density, including the finite temperature correction introduced by Langmuir [4]

$$J_{\rm CL} = \frac{4\epsilon_0}{9d^2}\left(\frac{-2q}{m}\right)^{1/2} V_{\rm A}^{3/2}(1 + 2.66(kT/(-qV_{\rm A}))^{1/2}). \tag{14}$$

We see in Fig. 2 the effects of both space charge, which is responsible for the sharp knee in the curves for small magnetic fields, and of magnetic field, which is responsible for the sharp reduction in the anode current as the magnetic field approaches $B_{\rm H}$.

Another interesting way to illustrate the separate effects of space charge and magnetic field is to plot the anode current normalized to the emitted current $J_{\rm RD}$, as shown in Fig. 3. Here, we see that, for low temperatures and small magnetic field, all of the emitted current reaches the anode. As temperature is increased and space charge density increases, some of the emitted current returns to the cathode due to the presence of a potential minimum near the cathode surface. As the magnetic field is increased, an increasing amount of current is reversed by the magnetic field.

Near the rollover point, or knee, in the curves of Figs. 2 and 3, where the transition from temperature-limited to space-charge-limited emission starts to occur, a potential minimum is forming in front of the cathode due to the density of the emitted space charge. This potential minimum implies a reversal of the electric field at the cathode surface. Only those particles with sufficient launch energy can get past the potential minimum and reach the anode. Fig. 4 shows the normalized electric field at the cathode surface as a function of temperature for the same values of magnetic field used in Figs. 2 and 3. We note that the electric field at the cathode under space charge-limited conditions approaches that of the vacuum field in magnitude, but with opposite sign.

Figs. 5 and 6 show the dependence of the potential minimum and its location as functions of temperature.

Fig. 7 illustrates the sharp reduction of current as the magnetic field approaches the Hull field, for various values of cathode temperature.

Fig. 8 illustrates the dependence of the anode current density on the anode voltage, for two values of magnetic field and three values of temperature. The dashed curves in Fig. 8 join the solid curves at values of anode voltage $V_{\rm A}$ at which all electrons emitted from the cathode reach the anode. It is notable that the anode current density may significantly exceed the Child–Langmuir value for very low anode voltages—deep into the space charge-limited regime. This is due to the Maxwellian distribution of initial velocities. Clearly, in the case that $V_{\rm A} = 0$, $J_{\rm CL} = 0$, some electrons in the tail of the distribution will still make it across the gap to the anode.

IV. PIC Simulations

We have used the PIC code XPDP1 [21] to analyze electron transport in a crossed-field gap as B increases from zero to

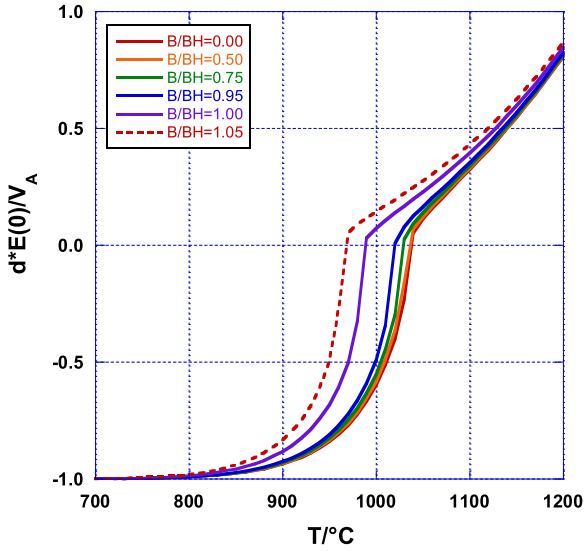

Fig. 4. Normalized electric field at the cathode versus temperature for various values of B/B_{H}.

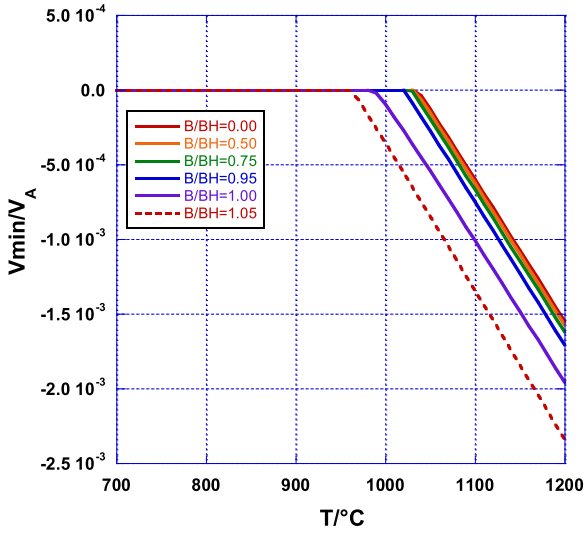

Fig. 5. Minimum potential versus temperature for various values of B/B_{H}.

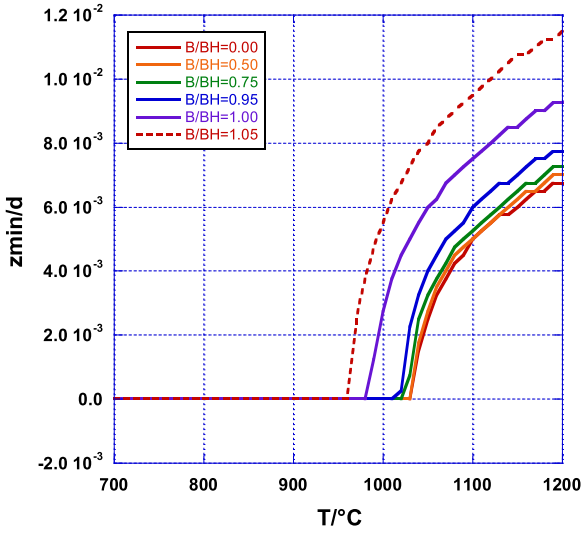

Fig. 6. Location of minimum potential versus temperature for various values of B/B_{H}.

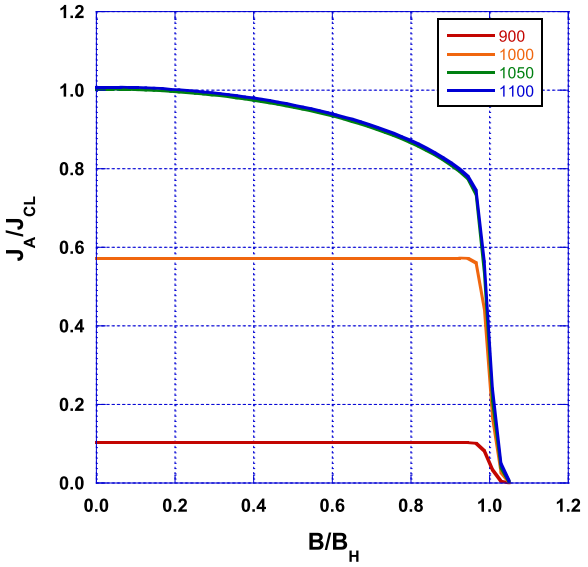

Fig. 7. Normalized anode current versus normalized magnetic field, for various values of cathode temperature (°C).

beyond B_{H}. XPDP1 is an electrostatic, nonrelativistic code that solves Poisson's equation in 1-D, but allows electron motions in 3-D. In our simulations, electrons are emitted from the cathode with a Maxwellian velocity distribution with temperature T; the emission current density is set equal to the Richardson–Dushman law [see (2)] with a work function $\varphi = 2$ eV. To compare with the analytic theory in Section III, we ran the cases with $B/B_{\mathrm{H}} = 0$, 0.5, 0.75, 0.95, 1.00, and 1.05.

The PIC simulation results, represented by the data points in Fig. 2 for $B/B_{\mathrm{H}} = 0$, 0.5, 0.75, and 0.95 are virtually identical to the analytic theory based on solutions of the Vlasov–Poisson equations. In Fig. 2, we show the detailed comparison in the most demanding "knee" region, where transition of the anode current from temperature-limited to space charge-limited flow occurs.

For $B/B_{\mathrm{H}} = 1.00$ and 1.05, the simulation shows that the initially laminar electron flow breaks down into a turbulent state even at very low temperatures, at which the Richardson–Dushman current density is only a small fraction of the Child–Langmuir value. For $B/B_{\mathrm{H}} > 1$, even at low temperatures, there is a potential minimum in this turbulent state, caused by the accumulation of space charge. This accumulation is a result of the failure to return to the cathode surface of electrons emitted with a very low emission velocity in the Maxwellian distribution [13], [14]. In contrast, the extended Fry–Langmuir theory does not show a potential minimum at low temperature (see Fig. 4). The different states exhibited in the PIC code results prevent a comparison with the steady-state theory for $B/B_{\mathrm{H}} > 1$.

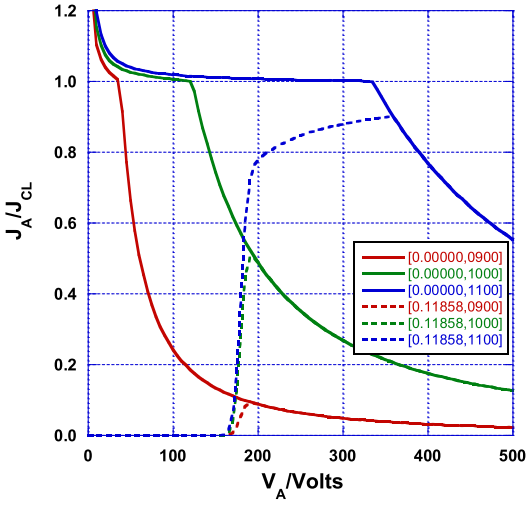

Fig. 8. Normalized anode current versus anode voltage, for various values of temperature and magnetic field. The legend is [B (Tesla), T (°C)]. The value $B = 0.11858$T is the Hull cutoff for our base case voltage $V_A = 179.5$ V.

V. Summary and Conclusion

This article extends the diode theory of Fry and Langmuir to include a transverse magnetic field B, ranging from zero to beyond the Hull cutoff magnetic field B_H. The electrons are emitted from the cathode with a Maxwellian velocity distribution, which is normalized according to the Richardson–Dushman law. The steady-state solutions are obtained semianalytically; these solutions include a potential minimum when the emitted current becomes large. Our theory reproduces Langmuir and Fry's results in the limit $B = 0$. For $B > B_H$, the anode current is practically zero, consisting only of electrons in the tail of the velocity distribution. These semianalytic, time independent solutions have been obtained for all values of B, including $B = B_H$.

The theoretical results are found to be in excellent agreement with PIC simulation for all test cases with $B < B_H$. For $B > B_H$, however, our simulations show that the initially laminar cycloidal electron orbits break down into Brillouin ($E \times B$) flow embedded in a turbulent background, even at a very low cathode temperatures, at which the emission current density is substantially less than the Child–Langmuir value. In fact, no current threshold for this breakdown was found; all cases tested resulted in turbulent behavior. We did investigate the possibility that low cathode temperatures (750 °C) as well as high magnetic fields ($B/B_H = 10$) could suppress turbulence. However, we found that lowering the cathode temperature and/or increasing the magnetic field only increased the formation time for the instability, but did not prevent it. Clearly, the transition region, $B \approx B_H$, requires further study.

This study is yet another among many [13]–[15], [22] that support the notion [14], [17], [18] that Brillouin-like flow, not cycloidal orbital states, is the preferred state for a magnetically insulated ($B > B_H$) diode. This is important since the different type of orbits (Brillouin versus cycloidal) yield very different results for the Buneman–Hartree synchronism condition for a cylindrical magnetron [23].

We remark that we cannot completely rule out the possibility, though it is unlikely in our view, that the transition to turbulence observed in PIC simulations is a numerical effect, due to intrinsic limitations of the PIC model. We do note that stable cycloidal orbits can be obtained with a mono-energetic electron beam in PIC simulations, provided the current is below a critical value [13]. Additionally, our larger point that cycloidal flow may be easily disrupted and transition to Brillouin-like flow is almost certainly true in a physical diode where many types of potentially destabilizing effects are present.

VI. Appendix
Calculation of Charge Density

The charge density to be used in Poisson's equation is given by (7) in the text, where the limits of integration are the ranges of particle initial values (u, ξ) that allow the particle to reach location $\bar{z}$. To determine these ranges, we note that the denominator in the integrand of (7) is $|v_z|/v_{th}$. In order for a particle to reach $\bar{z}$, we must have $v_z^2 \geq 0$, that is, $\xi \geq \xi_0(u; \bar{z}')$ for all $0 \leq \bar{z}' \leq \bar{z}$. This leads us to the definition

$$\xi^-_{0,\max} \equiv \max_{0 \leq \bar{z}' \leq \bar{z}} (\xi_0(u; \bar{z}')). \tag{A-1}$$

We find it convenient to define

$$\xi_1^-(u; \bar{z}) \equiv max(\xi^-_{0,\max}, 0). \tag{A-2}$$

All particles with $\xi \geq \xi_1^-(u; \bar{z})$ will reach $\bar{z}$ from the cathode with positive v_z. The contribution of these particles to the normalized charge density at $\bar{z}$ is therefore given by

$$\begin{aligned}\bar{\rho}^-(\bar{z}) &= \int_{-\infty}^{\infty} du \int_{\xi_1^-(u;\bar{z})}^{\infty} d\xi \frac{e^{-(\frac{u^2}{2}+\xi)}}{(\xi - \xi_0(u;\bar{z}))^{1/2}} \\ &= \pi^{1/2} \int_{-\infty}^{\infty} du e^{-u^2/2-\xi_0(u;\bar{z})} erfc[(\xi_1(u;\bar{z}) - \xi_0(u;\bar{z}))^{1/2}]\end{aligned} \tag{A-3}$$

where *erfc* is the complimentary error function.

A particle reaching $\bar{z}$ from the cathode may either continue on to reach the anode, or turn around at some value of $\bar{z}'$ satisfying $1 > \bar{z}' > \bar{z}$ and return to $\bar{z}$ (and then to the cathode). The initial conditions of particles returning to $\bar{z}$ will satisfy $\xi_1^+(u; \bar{z}) \geq \xi \geq \xi_1^-(u; \bar{z})$, where

$$\xi_1^+(u; \bar{z}) \equiv max(\xi^+_{0,\max}, 0) \tag{A-4}$$

and

$$\xi^+_{0,\max} \equiv \max_{\bar{z} \leq \bar{z}' \leq 1} (\xi_0(u; \bar{z}')). \tag{A-5}$$

The contribution of these particles to the charge density is

$$\begin{aligned}\bar{\rho}^+(\bar{z}) &= \int_{-\infty}^{\infty} du \int_{\xi_1^-(u;\bar{z})}^{\xi_1^+(u;\bar{z})} d\xi \frac{e^{-(\frac{u^2}{2}+\xi)}}{(\xi - \xi_0(u;\bar{z}))^{1/2}} \\ &= \pi^{1/2} \int_{-\infty}^{\infty} du e^{-u^2/2-\xi_0(u;\bar{z})} \\ &\quad \times \{erfc[(\xi_1^-(u;\bar{z}) - \xi_0(u;\bar{z}))^{1/2}] \\ &\quad - erfc[(\xi_1^+(u;\bar{z}) - \xi_0(u;\bar{z}))^{1/2}]\}\end{aligned} \tag{A-6}$$

if $\xi_1^+(u; \bar{z}) > \xi_1^-(u; \bar{z})$; $\bar{\rho}^+(\bar{z}) = 0$ otherwise, that is, if no particles return to $\bar{z}$.

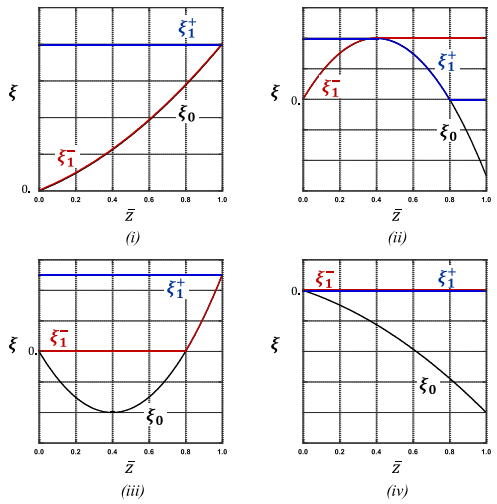

Fig. A-1. $\xi_1^-(u;\bar{z})$ (red) and $\xi_1^+(u;\bar{z})$ (blue) as functions of $\bar{z}$ for four different functions $\xi_0(u;\bar{z})$ (black), for a fixed value of u.

Plots of the quantities $\xi_0(u;\bar{z})$ and $\xi_1^{\pm}(u;\bar{z})$ as functions of $\bar{z}$ for fixed u are shown in Fig. A-1, for some simple illustrative cases. It is useful, in this figure, to think of an electron as a ball launched with an initial energy ξ that rolls along the landscape described by $\xi_0(u;\bar{z})$ (in black, in the figure). So for case (i) in the figure, for example, all electrons with energies $\xi > \xi_0(u;1) = \xi_1^+(u;\bar{z})$ reach the anode, while those with energies $\xi < \xi_1^+(u;\bar{z})$ return to the cathode.

Finally using (A-3) and (A-6), we state Poisson's equation in normalized variables

$$\frac{d^2\bar{V}(\bar{z})}{d\bar{z}^2} = \bar{J}_{\mathrm{RD}}(\bar{\rho}^-(\bar{z}) + \bar{\rho}^+(\bar{z})) \tag{A-7}$$

where $\bar{J}_{\mathrm{RD}} \equiv J_{\mathrm{RD}}d^2/(2\epsilon_0 v_{\mathrm{th}} V_{\mathrm{A}})$.

ACKNOWLEDGMENT

The authors acknowledge Dr. De-Qi Wen of Michigan State University for his assistance with the XPDP1 simulations.

REFERENCES

[1] O. W. Richardson, *The Emission of Electricity from Hot Bodies*. London, U.K.: Longmans, Green, and Company, 1916.
[2] S. Dushman, "Electron emission from metals as a function of temperature," *Phys. Rev.*, vol. 21, no. 6, pp. 623–636, Jun. 1923, doi: 10.1103/PhysRev.21.623.
[3] C. Child, "Discharge from hot CaO," *Phys. Rev. (Ser. I)*, vol. 32, p. 492, May 1911, doi: 10.1103/PhysRevSeriesI.32.492.
[4] I. Langmuir, "The effect of space charge and initial velocities on the potential distribution and thermionic current between parallel plates," *Phys. Rev.*, vol. 21, no. 4, p. 419, Apr. 1923, doi: 10.1103/PhysRev.21.419.
[5] T. Fry, "The thermionic current between parallel plane electrodes; velocities of emission distributed according to Maxwell's law," *Phys. Rev.*, vol. 17, no. 4, p. 441, Apr. 1921, doi: 10.1103/PhysRev.17.441.
[6] C. K. Birdsall and W. B. Bridges, *Electron Dynamics of Diode Regions*. New York, NY, USA: Academic, 1966.
[7] R. C. Davidson, *Physics of Nonneutral Plasmas*. Redwood City, VA, USA: Addison-Wesley, 1990.
[8] J. W. Luginsland, S. McGee, and Y. Y. Lau, "Virtual cathode formation due to electromagnetic transients," *IEEE Trans. Plasma Sci.*, vol. 26, no. 3, pp. 901–904, Jun. 1998.
[9] D. Chernin, Y. Y. Lau, J. Petillo, S. Ovtchinnikov, D. Chen, A. Jassem, R. Jacobs, D. Morgan, and J. Booske, "Effect of nonuniform emission on Miram curves," *IEEE Trans. Plasma Sci.*, vol. 48, no. 1, pp. 146–155, Jan. 2020.
[10] M. J. Cattelino, G. V. Miram, and W. R. Ayers, "A diagnostic technique for evaluation of cathode emission performance and defects in vehicle assembly," in *IEDM Tech. Dig.*, San Francisco, CA, USA, Dec. 1982, pp. 36–39, doi: 10.1109/IEDM.1982.190205.
[11] A. Hull, "The effect of a uniform magnetic field on the motion of electrons between coaxial cylinders," *Phys. Rev.*, vol. 18, no. 1, pp. 31–57, 1921, doi: 10.1103/PhysRev.18.31.
[12] Y. Y. Lau, P. Christenson, and D. Chernin, "Limiting current in a crossed-field gap," *Phys. Plasmas*, vol. 5, no. 12, pp. 4486–4489, 1993.
[13] P. Christenson and Y. Y. Lau, "Transition to turbulence in a crossed-field gap," *Phys. Plasmas*, vol. 1, no. 12, pp. 3725–3727, 1994. [Erratum, vol. 3, no. 11, p. 4293, 1996.]
[14] P. Christenson, D. Chernin, A. Garner, and Y. Y. Lau, "Resistive destabilization of cycloidal electron flow and universality of (near-) Brillouin flow in a crossed-field gap," *Phys. Plasmas*, vol. 3, no. 12, p. 4455, 1996, doi: 10.1063/1.872064.
[15] M. Lopez, Y. Y. Lau, J. Luginsland, D. Jordan, and R. Gilgenbach, "Limiting current in a relativistic diode under the condition of magnetic insulation," *Phys. Plasmas*, vol. 10, no. 11, p. 4489, 2003.
[16] R. V. Lovelace and E. Ott, "Theory of magnetic insulation," *Phys. Fluids*, vol. 17, no. 6, p. 1263, 1974, doi: 10.1063/1.1694876.
[17] J. Slater, *Microwave Electronics*. New York, NY, USA: Van Nostrand, 1951, p. 302.
[18] O. Buneman, "Symmetrical states and their breakup," in *Crossed-Field Microwave Devices*. New York, NY, USA: Academic, 1961, p. 218.
[19] M. Clark, B. Marder, and L. Bacon, "Magnetically insulated transmission line oscillator," *Appl. Phys. Lett.*, vol. 52, no. 1, p. 78, 1988.
[20] R. D. McBride *et al.*, "A primer on pulsed power and linear transformer drivers for high energy density physics applications," *IEEE Trans. Plasma Sci.*, vol. 46, no. 11, pp. 3928–3967, Nov. 2018.
[21] J. P. Verboncoeur, M. V. Alves, V. Vahedi, and C. K. Birdsall, "Simultaneous potential and circuit solution for 1D bounded plasma particle simulation codes," *J. Comput. Phys.*, vol. 104, no. 2, pp. 321–328, Feb. 1993.
[22] A. Palevsky and G. Bekefi, "Microwave emission from pulsed, relativistic e-beam diodes. II. The multiresonator magnetron," *Phys. Fluids*, vol. 22, no. 5, p. 986, 1979, doi: 10.1063/1.862663.
[23] Y. Y. Lau, J. Luginsland, K. Cartwright, D. Simon, W. Tang, B. Hoff, and R. Gilgenbach, "A re-examination of the Buneman–Hartree condition in a cylindrical smooth-bore relativistic magnetron," *Phys. Plasmas*, vol. 17, no. 3, 2010, Art. no. 033102.

David Chernin received the Ph.D. degree in applied mathematics from Harvard University, Cambridge, MA, USA, in 1976.

He has been with Leidos, Reston, VA, USA, and its predecessor company SAIC since 1984, where he has conducted research on beam-wave interactions and other topics in the physics of particle accelerators and vacuum electron devices.

Abhijit Jassem received the B.S. degree in nuclear engineering from Purdue University, West Lafayette, IN, USA, in 2016. He is currently pursuing the Ph.D. degree with the University of Michigan's Nuclear Engineering and Radiological Sciences Program, Ann Arbor, MI, USA.

He is working with the Plasma, Pulsed Power, and Microwave Laboratory, University of Michigan.

Y. Y. Lau (Fellow, IEEE) received the S.B., S.M., and Ph.D. degrees in electrical engineering from the Massachusetts Institute of Technology (MIT), Cambridge, MA, USA.

He is currently a Professor with the University of Michigan, Ann Arbor, MI, USA, specialized in RF sources, heating, and discharge.

Dr. Lau received the 1999 IEEE Plasma Science and Applications Award and the 2017 IEEE John R. Pierce Award for Excellence in Vacuum Electronics. He is an APS Fellow.